EFFECTS OF SOIL TEMPERATURE ON A COUPLED PHOTOSYNTHESIS-STOMATAL CONDUCTANCE MODEL FOR FOUR BOREAL TREE SPECIES

Tiebo Cai ©

FACULTY OF FORESTRY AND THE FOREST ENVIRONMENT
LAKEHEAD UNIVERSITY
THUNDER BAY
ONTARIO

ProQuest Number: 10611928

LIBRARY RIGHTS STATEMENT

ABSTRACT

Tiebo, Cai. 2000. Effects of soil temperature on a coupled photosynthesis-stomatal conductance model for four boreal species. (68p). Supervisor: Dr. Qing-lai, Dang.

Keywords: Soil temperature, modeling, photosynthesis, stomatal conductance, aspen, jack pine, black spruce, white spruce.

In order to examine the effects of soil temperature on a coupled photosynthesis-stomatal conductance model, seedlings of trembling aspen (*Populus tremuloides* Michx), jack pine (*Pinus banksiana* Lamb.), black spruce (*Picea Mariana* (Mill) B.S.P.) and white spruce (*Picea glauca* (Moench) Voss.) were grown over a wide range of soil temperatures from 5 °C to 35 °C. Temperature, light and CO_2 response curves of foliar gas exchange were measured four months after the start of the treatment. The results showed that the four boreal tree species had very similar cardinal soil temperatures for key model parameters (i.e., V_{cmax}, J_{max}). The key parameters of the model showed dual soil temperature symmetry: below-ground and above-ground temperature symmetry, and low and high temperature symmetry. In the below-ground and above-ground temperature symmetry, the key model parameters responded to soil temperature in a similar manner as to leaf temperature. For low and high soil temperature symmetry, the symmetry was not perfect, with steeper slope at the higher-than-optimum temperature range, which indicated the photosynthetic machinery of the four boreal trees was suppressed more at high soil temperatures than at low soil temperatures.

The effects of soil temperature on key model parameters were modeled using three different equations. Three equations fitted the measured key model parameters well, but only the bio-chemical equation showed a specific pattern for the equation parameters between the four species. Soil temperature had no effects on R_d, the daytime respiration that continues in light. It was speculated that after four months of soil temperature treatments, the four boreal tree species acclimated to different soil temperature conditions by optimizing allocation of nitrogen investment into different functional photosynthetic components and balancing water use efficiency and nitrogen use efficiency.

TABLE OF CONTENTS

LIST OF TABLES

LIST OF FIGURES

ACKNOWLEDGMENTS

I am greatly indebted to my supervisor, Dr. Qinglai Dang for his great insights and substantial help on my thesis. He walked me every step during the two-year study and did more than his share.

I would like to thank my committee members: Dr. Gary Murchison of Lakehead University; Dr. Changhui Peng of Ontario Forest Research Institute and the External Examiner, Dr. Ted Hogg of Canadian Forest Service, for their valuable comments and inputs.

I wish to thank Dr. Kenneth Brown and Dr. Len Meyer for their sincere help during my thesis writing process.

My thanks also go to some of my Chinese friends for their warm help and enthusiastic encouragement.

I would like to express my gratitude to my parents, brother and sisters for their moral support and inspiration.

Special thanks are reserved for my wife and my daughter. They have been through too much in order to support my study. They have given me a new perspective of life.

INTRODUCTION

The boreal forest covers approximately 14.7 million km^2, 11% of the earth's surface, and is one of the largest terrestrial ecosystem on earth (Bonan and Shugart 1989). Its ecophysiological process can have a profound impact on the environmental conditions of the earth's surface (Keeling et al. 1996). For example, the photosynthetic activity of this ecosystem can explain 30% of the annual variation in atmospheric CO_2 concentration. Tree transpiration significantly influences the water flux from the boreal forest (Dang et al. 1998) and the properties of the lower atmosphere (Margolis and Ryan 1997). Recent studies, however, suggest that the climate change associated with increasing atmospheric CO_2 will be most prominent in the boreal forest region (Tans et al. 1990; Sellers et al. 1997). The response of the boreal forest to the global change will be of significance to the future climatic conditions in the world. Furthermore, global climate change is likely to trigger a series of changes in the soil and aboveground environment, especially soil temperature. The soil temperature change might result in alterations in the vegetation limits, immigration or suppression of certain species in the boreal forests (Larcher 1995).

Computer modeling is a powerful tool for investigating interrelationships between physiological processes and for summarizing and understanding complex ecophysiological processes and their responses to environmental factors (Sellers et al. 1996; Dang et al. 1997). A coupled photosynthesis and stomatal conductance model (A – g_s model) is often used to summarize the biochemical processes of photosynthesis and

their responses to environmental conditions (Farquhar et al. 1980; Collatz et al. 1991) and to scale photosynthesis and stomatal conductance in space and time (Sellers et al. 1996). However, the parameters of this kind of model are generally derived from data collected under constant soil conditions (Dang et al. 1997). Although models are available for predicting soil temperature, it is difficult to incorporate them into ecophysiological models, such as the $A - g_s$ model, because of the lack of information on how soil temperature affects model parameters and ecophysiological responses to soil temperature. This lack of information limits the accuracy of ecophysiological models, particularly when applied to areas with distinctly different soil temperatures or when incorporated into larger-scale models (Sellers et al. 1996). For example, the soil temperature in boreal forest is complex and highly variable. It ranges from permafrost to warm in south facing slopes and newly burned sites (Bonan and Shugart 1989). So when the A-g_s model is applied to the vast area of boreal forests, it is necessary to take soil temperature into consideration.

The objectives of this study were to investigate the physiological response of boreal tree species to soil temperature change , and to formulate the relationship of ecophysiological parameters to soil temperature. The algorithms for considering soil temperature in the A-g_s model will make it possible to integrate soil temperature models into this model to increase its accuracy and applications in different geographic areas. The algorithms also will improve the accuracy of large-scale canopy process models which incorporate the A-g_s model for studying interactions between the boreal ecosystem and the atmosphere.

This paper parameterized and tested the photosynthesis model proposed by Farquhar et al. (1980) and the stomatal conductance model proposed by Ball et al. (1987) for four boreal tree species grown under a wide range of soil temperatures. Furthermore, the relationships between key model parameters and soil temperature were formulated, and incorporated into Farquhar's C_3 photosynthesis model for boreal tree species as separate modules.

The study tested the hypothesis that when grown under different soil temperatures, boreal tree species had dual temperature symmetry: (1) above-ground and below-ground temperature symmetry, and (2) low and high temperature symmetry. In this study, seedlings were exposed to a range of soil temperatures (below-ground temperature) from 5 °C to 35°C, but to the same ambient air temperature (above-ground temperature). We hypothesized that the ecophysiological parameters would respond to the soil temperature in the same manner as if soil temperature were kept constant while leaf temperature were increased from 5 °C to 35 °C. For the low and high temperature symmetry, we hypothesized that the soil temperature response curves of ecophysiological parameters were symmetric, i.e., the two halves of the response curve along the optimum temperature were the mirror image of each other.

MODEL DESCRIPTION

The coupled photosynthesis-stomatal conductance model used was derived from the photosynthesis model of Fraquhar et al. (1980). The fundamental assumptions underlying this model for C_3 photosynthesis are (1) photosynthesis may be explained on the basis of Rubisco activity, and (2) Rubisco activity is entirely limited either by RuBP concentration or, if RuBP is saturating, by the kinetic properties of Rubisco as modulated by the competition between CO_2 and O_2 (Harley and Tenhunen 1991). In this model, net CO_2 assimilation (A) is the result of the rate of carboxylation (V_c) minus photo-respiration and other respiratory processes.

$$A = V_c - 0.5V_o - R_d = V_c \cdot (1 - 0.5\frac{V_o}{V_c}) - R_d \qquad [1]$$

Where V_c and V_o are the rates of RuBP carboxylation and oxygenation respectively, and R_d (daytime respiration) is the rate of CO_2 evolution from processes other than photorespiration (i.e., mitochondrial respiration from non-autotrophic tissue of the leaf and mitochondrial respiration in autotrophic cells that continues in the light). Number 0.5 denotes that one CO_2 is produced per two oxygenation reactions during the photo-respiration.

V_o/V_c, when expressed in terms of the enzyme specificity factor, τ, is:

$$\frac{V_o}{V_c} = \frac{O}{\tau \cdot C_i} \qquad [2]$$

Where O and C_i are the concentrations of O_2 and CO_2 at the site of fixation. The factor τ

may be further expressed in terms of enzyme kinetic parameters as follows:

$$\tau = \frac{V_{c\,max} \cdot K_o}{V_{o\,max} \cdot K_c} \qquad [3]$$

Where V_{cmax} and V_{omax} are the maximum rates and K_c and K_o are Michaelis-Menten

constants for carboxylation and oxygenation, respectively.

To be consistent with the terminology developed by Farquhar, Γ_* is used to express the

CO_2 compensation point in the absence of R_d. Γ_*, when expressed in terms of kinetic

parameters, is inversely related to τ:

$$\Gamma_* = \frac{0.5 \cdot O \cdot V_{c\,max} \cdot K_c}{V_{o\,max} \cdot K_o} = \frac{0.5 \cdot O}{\tau} \qquad [4]$$

Making the appropriate substitutions using Eq.[3]&Eq.[4], Eq.[1] may be rewritten as:

$$A = Vc \cdot (1 - \frac{\Gamma_*}{C_i}) - R_d \qquad [5]$$

As discussed above, V_c is limited either by the activity of Rubisco (assuming RuBP is saturating) or by the rate of RuBP regeneration mediated by the rate of electron-transport. Thus, $V_c = \min\{W_c, W_j\}$, where $\min\{\}$ denotes the minimum of W_c (Rubisco-limited rate of carboxylation) and W_j (RuBP-limited rate of carboxylation when RuBP regeneration is limited by electron transport) (Harley and Tenhunen 1991).

Thus,

$$A = (1 - \frac{\Gamma_*}{C_i}) \min\{W_c, W_j\} - R_d \qquad [6]$$

The relationship described in Eq.[6] in the CO_2 response curve of photosynthesis (abbreviated as A/C_i curve) is shown in Figure 1.
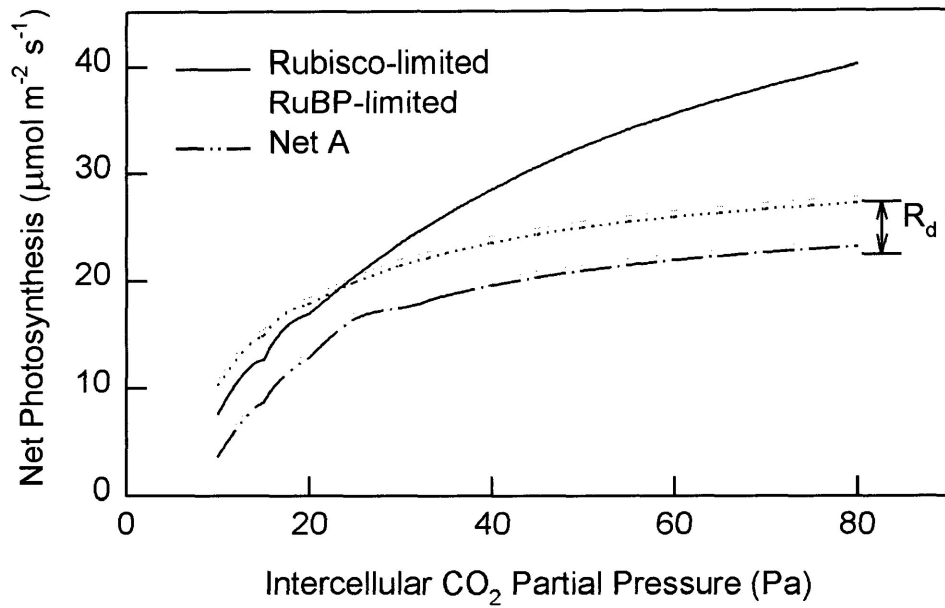
Figure 1. Schematic description of photosynthesis model behavior. Net A is the minimum of two functions minus R_d: one is the Rubisco limited rate of carboxylation and the other is the RuBP limited rate of carboxylation. R_d is the respiration that continues in the light.

W_c is assumed to obey competitive Michaelis-Menten kinetics. So,

$$W_c = \frac{V_{c\,max} \cdot C_i}{C_i + K_c(1 + \frac{O}{K_o})}$$ [7]

Incorporating Eq. [4] into Eq. [2],

$$\frac{V_o}{V_c} = \frac{2\Gamma_*}{C_i}$$ [8]

In the RuBP-limited part of the A/C_i curve (i.e., at high C_i), the rate of electron transport (J) is constant (Figure 1). Increasing the partial pressure of CO_2 increases the rate of carboxylation at the expense of the rate of oxygenation. There is a minimum requirement of four electrons per carboxylation or oxygenation reaction. Hence, the minimum electron transport rate (J) required for particular rates of carboxylation and oxygenation

$$J = 4 \cdot (V_c + V_o)$$ [9]

Combining Eq. [8] and Eq. [9], the RuBP-limited rate (or ET-limited rate) of carboxylation can then be expressed as:

$$W_j = \frac{J \cdot C_i}{4(C_i + 2\Gamma_*)}$$ [10]

The only light dependency in the model is electron transport. Based on Smith (1937),

Tenhunen et. al. (1976) and Harley et. al. (1992):

$$J = \frac{\alpha \cdot Q_p}{\sqrt{(1 + \frac{\alpha^2 \cdot Q_p^2}{J_{max}^2})}} \qquad [11]$$

Where α is the efficiency of light energy conversion on an incident light basis (mol

electrons/ mol photons), Q_p is photosynthetically active radiation (PAR) flux density,

and J_{max} is the light-saturated rate of electron transport.

The RuBP regeneration limited by the availability of inorganic phosphate (P_i) for

photophosphorylation (W_p) (Sharkey 1985) and the gradual transition (co-limitation)

from one limitation to another (Collatz et al. 1991) are not considered in the present

study.

Parameter values at 25 °C are normally given for the preceding models in

literature. Values for other temperatures can be determined from the temperature

dependency of the parameter. The temperature dependency of V_{cmax} or J_{max} is described

as follows (Johnson et al. 1942; Tenhunen et al. 1976; Harley and Tenhunen 1991):

$$Parameter = \frac{Parameter(T_{ref}) \cdot e^{\left[\frac{\Delta H_a}{R \cdot T_{ref}}(1 - \frac{T_{ref}}{T_k})\right]}}{1 + e^{(\frac{\Delta S \cdot T_k - \Delta H_d}{R \cdot T_k})}} \qquad [12]$$

Where Parameter refers to either V_{cmax} or J_{max} and Parameter (T_{ref}) is the potential value that this parameter would have at the reference temperature (T_{ref}) in the absence of any deactivation due to high temperature, ΔH_a is the energy of activation, ΔH_d is the energy of deactivation, ΔS is an entropy term, T_k is the absolute temperature of leaf, and R is the gas constant. T_{ref} normally is taken as 25 °C.

The temperature dependency of V_{cmax} or J_{max} may also be described by polynomial equations, Eq. [13] and Eq. [14] (Kirschbaum and Farquhar 1984).

$$V_{c\,max} = V_{c\,max\,25} \cdot [1 + 5.05 \times 10^{-1} \cdot (T_L - 25) - 2.48 \times 10^{-4} \cdot (T_L - 25)^2 \\ - 8.09 \times 10^{-5} \cdot (T_L - 25)^3] \qquad [13]$$

$$J_{max} = J_{max\,25} \cdot [1 + 4.09 \times 10^{-2} \cdot (T_L - 25) - 1.54 \times 10^{-3} \cdot (T_L - 25)^2 \\ - 9.42 \times 10^{-5} \cdot (T_L - 25)^3] \qquad [14]$$

Where T_L is leaf temperature in °C, V_{cmax25} is V_{cmax} at 25 °C, and J_{max25} is J_{max} at 25 °C.

In this paper, Eq. [12] was employed to determine the temperature dependency of V_{cmax} and J_{max}.

The temperature dependencies of τ, K_c, K_o, and R_d may each be described by an Arrhenius Equation:

$$\text{Parameter} = \text{Parameter}(T_{\text{ref}}) \cdot e^{\left[\frac{\Delta H_a}{R \cdot T_{\text{ref}}}(1 - \frac{T_{\text{ref}}}{T_k}) \right]} \qquad [15]$$

Where Parameter may represent τ, K_c, K_o, or R_d, and ΔH_a is the activation energy for the corresponding parameters.

To be useful for predicting leaf gas-exchange responses to varying environmental conditions, the models of CO_2 assimilation presented above must be integrated with a model describing stomatal conductance (g_s). Although the physiology of stomata has been extensively examined, a mechanistic understanding of how stomata respond to light, temperature, humidity, and CO_2 remains elusive. The often-noted correlation between stomatal conductance and net CO_2 assimilation (Wong et al., 1979) has led to the development of empirical models in which assimilation is a parameter used to predict conductance. Ball (1988) and Ball and Berry (1991) developed the following empirical model to describe stomatal conductance:

$$g_s = b + m \cdot 100 \cdot A \cdot \frac{h_s}{C_s} \qquad [16]$$

Where h_s and C_s are relative humidity (as a decimal) and CO_2 partial pressure at the leaf surface (i.e., inside the leaf boundary layer) respectively, b is the minimum stomatal conductance to H_2O when $A = 0$ at the light compensation point, and m is an empirical coefficient which represents the composite sensitivity of stomatal conductance to assimilation, CO_2 partial pressure, humidity and temperature. The factor 100 corrects for

the differences in the units of g_s and $A \cdot h_s/C_s$. Stomatal opening in response to PAR is controlled via A, which is considered to be related to the energy requirement for maintaining guard cell turgor (Falge et. al. 1996). The stomata of some species can also sense and respond to blue light (Tardieu and Davies 1993) and the decline of C_i associated with increasing PAR (Lasceve et. al. 1993, Lambers et. al. 1998). Effects of non-uniform stomatal closure (patchiness) on stomatal conductance are not considered in present study.

Stomatal conductance is thus dependent on A, while A is also dependent on g_s through g_s's effect on C_i, according to the following equation:

$$C_i = C_a - \frac{A \cdot 1.6 \cdot 100}{g_s} \qquad [17]$$

The factor 1.6 corrects for the difference in diffusivity between CO_2 and H_2O and the factor 100 is a conversion factor when A is in $\mu mol \ m^{-2} \ s^{-1}$ and g_s is in $mmol \ m^{-2} \ s^{-1}$

Given above interdependencies between g_s, C_i and A, the model must solve for C_i iteratively. Thus, A and g_s are integrated by iterating for the value of C_i that is compatible with both A (Eq. [6]) and g_s (Eq.[16]) predicted by the models, where A and g_s are related according to Eq.[17].

The iterative relationship between A, g_s and C_i is shown in Figure 2. The rate of CO_2 assimilation is given by the simultaneous solutions to three equations: (1) $A=f(C_i)$

(Eq.[6]), i.e., the demand function, which represents the biochemical limitation to CO_2 fixation, as graphically represented by an A/C_i curve; (2) $A=g_c(C_a-C_i)$ (Eq.[17]), the supply function, describing the diffusion of CO_2 gas from the atmosphere to the intercellular space. Graphically this is represented by a straight line originating from C_a on the x-axis and with slope $= -g_c$ ($g_c =$ conductance to CO_2); (3) the constraint function (Eq.[16]) links the above two equations. This function is not shown in this Figure 2. The intersection between the supply function and demand function gives the simultaneous solution to the three equations and A under that condition.
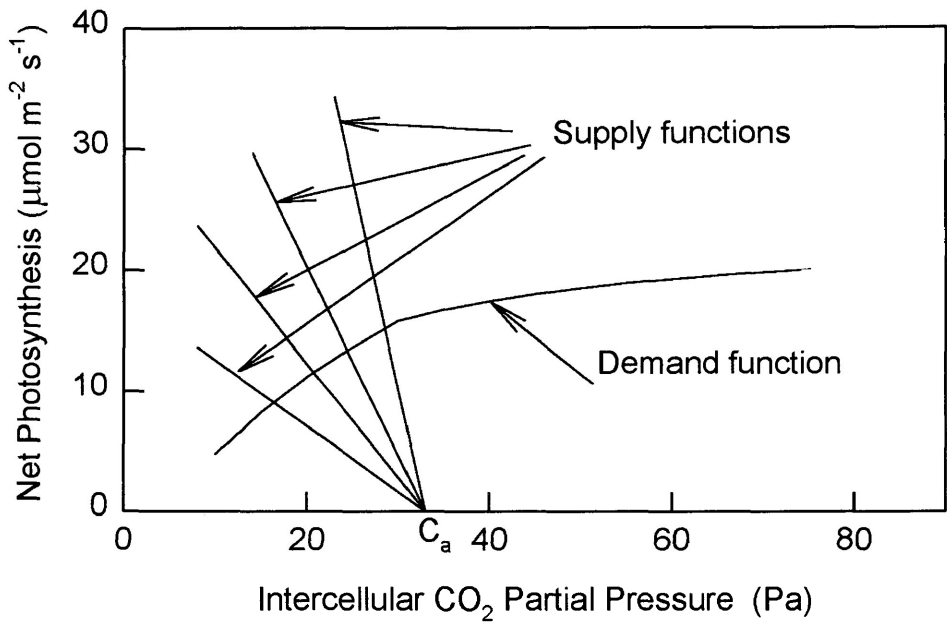
Figure 2. Modeled A/C_i relationship. The family of lines emanating from C_a represent different values of stomatal conductance.

MATERIALS AND METHODS

Plant Materials

One-year old seedlings of black spruce (*Picea Mariana* (Mill.) B.S.P.), white

spruce (*Picea glauce* (Moench) Voss.) and jack pine (*Pinus banksiana* Lamb.) were

obtained from A&R Container Tree Seedling Nursery in Dorion, Ontario. The seedlings

were dormant and stored in cool storage (2 °C) before the start of the experiment. Aspen

seedlings (*Populus tremuloides* Michx.) were grown from seeds in the Lakehead

University Greenhouses. The dormancy of aspen seedlings was induced at the end of the

fourth month by exposing them to 15/5 °C day/night temperatures and 8-hour

photoperiod. Aspen seedlings were also placed in cool storage before the initiation of the

experiment.

Experimental design

The study was carried out in a split block design with two greenhouses, seven soil

temperatures and four species. Each greenhouse contained all seven soil temperatures of

5, 10, 15, 20, 25, 30, and 35 °C. The soil temperatures were randomly assigned to each of

the soil temperature boxes in each greenhouse. Soil temperatures were controlled by

circulating temperature-controlled water around the seedling containers which were

contained in a plywood box. Eight rows of containers (14 in each row) were held in each

plywood box. Water was circulated through the space between containers. Each container

had one drainage hole to allow the free drain of water and fertilizer solution. To avoid the

leakage of the circulating water, the bottom of the container was sealed to the bottom of

the plywood box. The temperature of the circulating water was controlled using a refrigerated circulating water bath or a flow-through chiller or heater, depending on the soil temperature required. Each species was randomly assigned to two rows of the eight rows of containers in the plywood box. Soil temperature were monitored continuously throughout the experiment using a National Instrumentation SCXI MS 100 (National Instruments Corporation, Austin, Taxis, USA) connected to Pentium computer. The temperature measurements indicted that the soil temperatures were well controlled. $T_{soil} = 0.1202 + 0.9914*T_{water}$, $R^2 = 0.999$. T_{soil} and T_{water} refer to soil temperature and the temperature of the circulating water respectively.

Growing Conditions

The day and night temperatures in both greenhouses were controlled at 22.5 +0.6 and 14.3+0.3 S.E.M. $^{\circ}$C, respectively. The daytime temperature fluctuated more than night temperature and was generally above the set point on sunny days. The experiment started on February 6,1999. High-pressure sodium lamps were used to extend the natural photoperiod to 16 hours in the early part of the experiment. The growing medium used was a mixture of peat-moss and vermiculite 50/50 (v/v). All the seedlings were watered and fertilized to saturation every second day using a fertilization solution of 126ppm N, 44ppm P, 83ppm K, 40ppm Mg, 52ppm S, 30ppm Ca, 2.5ppm Fe, 0.67ppm Mn, 0.4ppm Zn, 0.3ppm Cu, 0.12ppm B, 0.003 ppm Mo (Landis 1989). The salinity and pH of the growing medium solution were measured at the end of each month using an AGRITEST pH and EC/TDS meter (HANNA Instruments, Portugal). The largest value of electrical

conductivity (EC) was 1.3 mS/cm, which is within the range (< 2.2 mS/cm) recommended by Landis et al. (1989). Soil pH was about 5.9 during the experiment.

Model Parameterization

For a complete parameterization of the model, the temperature dependencies of V_{cmax} and J_{max} (Eq. [12]), and of K_c, K_o, R_d and τ (Eq. [15]) need to be determined. Small but significant differences in K_c between C_3 plant species have been reported. (Keys 1986, Evans and Seeman, 1984). Values for K_c (in Pa) and K_o (in kPa) at 25 °C used in recent modeling efforts include the following: $K_c = 30$, $K_o = 16$ (Fraquhar and Wong 1984); $K_c = 31$, $K_o = 15.5$ (Kirschbaum and Farquhar 1984); $K_c = 30$, $K_o = 21.2$ (von Caemmerer and Fraquhar 1984); $K_c = 30$, $K_o = 30$ (Collatz et al. 1991, Dang et al 1998); and $K_c = 32.9$, $K_o = 39.7$ (Jordan and Ogren 1984). The temperature dependency values from Jordan and Ogren (1984) were chosen in this study (Table 1 and Figure. 3).
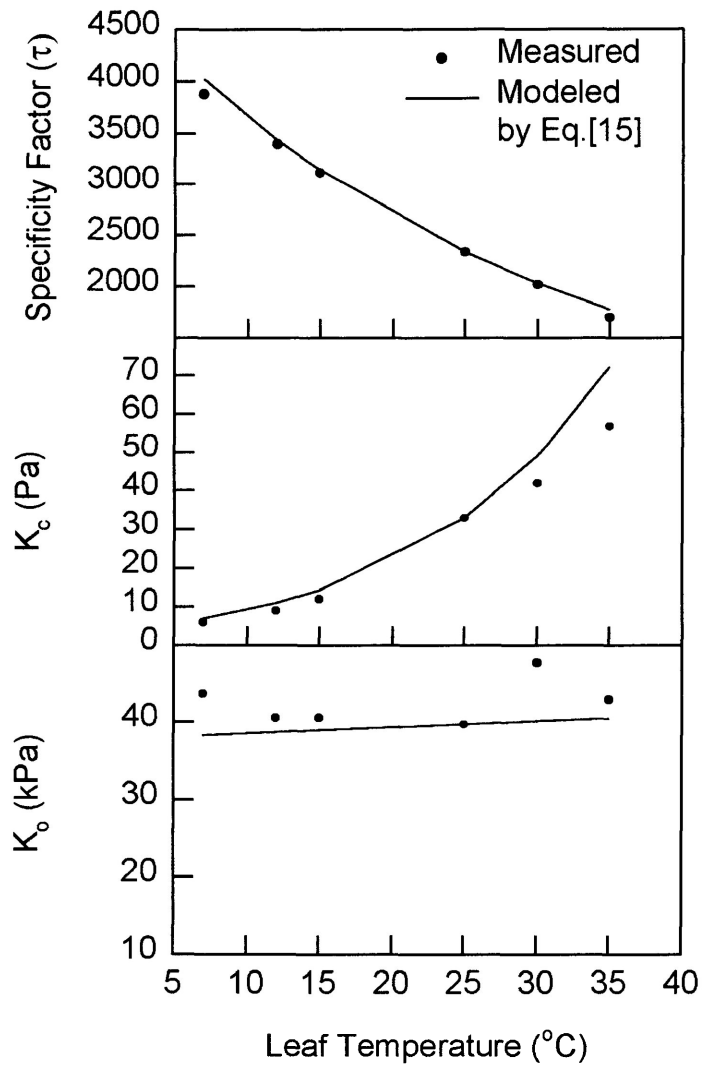
Figure 3. Temperature dependencies of τ, K_c and K_o.

The temperature dependency parameters (ΔH_a, ΔS, and ΔH_d), especially ΔH_a values for V_{cmax} and J_{max}, vary greatly across C_3 plants (Farquhar et al 1980; Harley and Tenhunen 1991; Harley et al 1992; Falge et al 1996; Walcroft et al 1997; Wohlfahrt et al 1998). The average values of these parameters available from the above literature were used in this study, because the activation energy (ΔH_a), deactivation energy (ΔH_d) and the entropy term (ΔS) are state functions (Chang 1994; Voet and Voet 1995), which means the three parameters should have the same values for all C_3 species due to their common photosynthetic pathways. The values are shown in Table 1 and Figure.4. In Figure.4(a) and 4(b), V_{cmax} and J_{max} were modeled by Eqs. [12], [13] and [14]. The temperature dependency of V_{cmax} and J_{max} in the absence of any deactivation due to high stressful temperature were also shown in Figure 4(a) and 4(b).
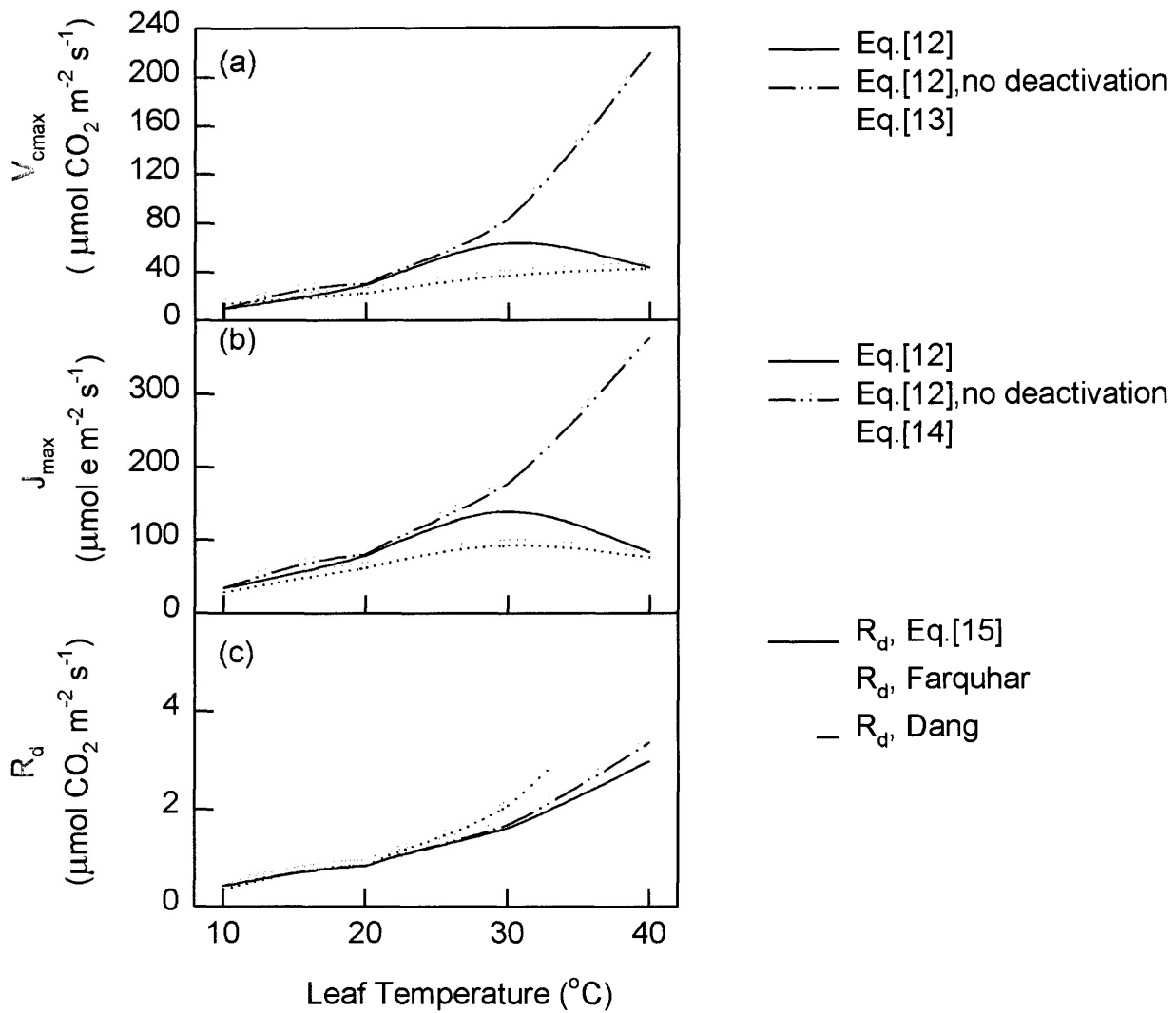
Figure 4. Temperature dependencies of V_{cmax}, J_{max} and R_d. In Figure 4(c), "R_d, Farquhar" refers to Farquhar et al. (1980) with Q_{10} =2.46, and "R_d, Dang" refers to Dang et al. (1998) with Q_{10} = 2.1.

Table 1. List of model parameters and their temperature dependency. The values were determined as described in the text. The reference temperature was at 298K.

Parameter	Units	Temperature parameters	Values	Units
K_c	Pa CO_2	ΔHa	59789	J mol⁻¹
K_o	kPa O_2	ΔHa	1397	J mol⁻¹
		ΔHa	-20970	J mol⁻¹
R_d	μmol CO_2 m⁻² s⁻¹	ΔHa	48294	J mol⁻¹
V_{cmax}	μmol CO_2 m⁻² s⁻¹	ΔHa	75794	J mol⁻¹
		ΔHd	202022	J mol⁻¹
		ΔS	657	J K⁻¹ mol⁻¹
J_{max}	μmol electrons m⁻² s⁻¹	ΔHa	58936	J mol⁻¹
		ΔHd	199233	J mol⁻¹
		ΔS	647	J K⁻¹ mol⁻¹

The apparent quantum yield at saturating CO_2, was determined through regression for the initial part of the light response curve of photosynthesis (PAR <200). The assumption that 4 mol electrons is sufficient to regenerate enough RuBP for CO_2 carboxylation gives α = 4*apparent quantum yield. The intercept of the regression was assumed to be the rate of dark respiration. R_d (daytime non-photorespiration) is taken to be half the magnitude of dark respiration (Wohlfahrt et al 1998).

$$R_d = 0.5 \cdot R_{dark}$$ [18]

At saturating PAR and C_i values below approximately 25Pa, RuBP levels are assumed to be saturating. Thus, the rate of carboxylation is limited solely by the amount, activity, and kinetic properties of Rubisco (i.e., W_c). By substituting Eq.[7] into Eq. [6], together with estimates of τ, K_c, K_o, O (20.9 kPa) and R_d, it is possible to estimate the V_{cmax} from the lower part of A/C_i curve by Eq. [19].

$$A = \frac{V_{c\,max} \cdot (C_i - \Gamma_*)}{C_i + K_c(1 + \dfrac{O}{K_o})} - R_d \qquad [19]$$

Having determined the V_{cmax} value from the lower part of the A/C_i curve, along with the α and R_d from the light response curve, non-linear least squares techniques were used to fit entire CO_2 response curve to Eq. [6] in order to determine best fit estimates of J_{max}. In this study, parameters (eg., V_{cmax}, J_{max}, R_d, α) were determined in a stepwise procedure, sequentially fixing the parameters which could be best estimated, and using these best estimated values to limit the range for variables to be determined.

The slope and intercept of the stomatal conductance equation in Eq. [16] were determined through linear regression from a plot of g_s versus (A·h_s/C_s), where g_s is allowed to vary with changes in PAR, C_s, leaf temperature and humidity.

Data Analysis

Parameter estimation was conducted using the Marquardt-Levenberg nonlinear regression algorithm in the curve-fitting program of SigmaPlot 2.0 for Windows (Jandel Scientific Inc., San Raphael, CA). To run the curving-fitting program, the parameters to be determined had to be assigned an initial estimated value. The program then sought the values for one or more parameters that best fit the data by minimizing the sum of the squared difference between the values of the observed and predicted values of the dependent variable (SS) (Dang et al. 1998).

$$SS = \sum_{i=1}^{n} (y_i - y_i^{\wedge})^2$$

where y_i is the observed and $y_i^{\wedge}$ is the predicted value of the dependent variable. Since the residuals for V_{cmax} and J_{max} was homogeneous across all soil temperature and species groups, no weighting to the residuals was used in the curve-fitting procedure. To compare the fitting effects of different models, norm in the program were used as a gauge to check the model fitness.

$$Norm = \sqrt{SS}$$

The smaller the norm value, the better the fit.

Statistical analysis was conducted in DataDesk 6.0 (Data Description, Inc., 1996, NY). The linear model for this study was listed in Appendix II. Analysis of Variance

(ANOVA) was performed to test the null hypotheses (P = 0.05). As in most statistical

analyses, the ANOVA assumptions (i.e., residuals in the linear model are independently

and identically distributed in a normal distribution with mean zero) were examined. Since

the data met the ANOVA assumption reasonably well, no transformation of the raw data

was executed. Insignificant interaction effects were pooled based on the critical value P =

0.25. When interaction effects were significant, investigated the highest order interactions

that were significant before examining lower order interactions or main effects (Brown

1995).

RESULTS

Effects of soil temperature on V_{cmax}

In general, V_{cmax} in each species increased exponentially with increasing soil

temperature from 5 °C to the optimum temperatures (most of them were at 25 °C), then

decreased exponentially (Figures 5 a-d). Three equations were used to model the

relationship between V_{cmax} and soil temperature.

$$V_{c\,max} = a_1 + b_1 \cdot T_s + c_1 \cdot T_s^2 + d_1 \cdot T_s^3 \qquad\qquad [20]$$

$$V_{c\,max} = V_{c\,max\,25} \cdot [1 + a_2 \cdot (T_s - 25) + b_2 \cdot (T_s - 25)^2 + c_1 \cdot (T_s - 25)^3] \qquad [21]$$

$$V_{c\,max} = \frac{V_{c\,max\,25} \cdot e^{\left[\frac{\Delta Ha}{R \cdot 298} \cdot (1 - \frac{298}{T_s})\right]}}{1 + e^{\left[\frac{\Delta S \cdot T_s - \Delta Hd}{R \cdot T_s}\right]}} \qquad\qquad [22]$$

where a_1, b_1, c_1, a_2, b_2, and c_2 are coefficients in Eq.[20] and Eq.[21]. In Eq.[22], ΔH_a is

the activation energy, ΔH_d is the deactivation energy, ΔS is an entropy term, T_s is the soil

temperature in °C or K according to the equations used, and R is the gas constant. V_{cmax25}

is the mean value of V_{cmax} at 25 °C. Eq.[21] was adopted from the equation in

Kirschbaum and Farquhar (1984) for air temperature, and Eq. [22] from Harley et. al.

(1992). The coefficients for the above equations were listed in Tables 2 to 5.

Table 2. Coefficients of V_{cmax} for Eq. [20]

Species	a_1	b_1	c_1	d_1
Aspen	35.83	-1.99	0.27	-0.006
Jack pine	2.25	1.78	0.06	-0.0029
Black spruce	15.61	-0.24	0.14	-0.0038
White spruce	6.34	1.72	0.02	-0.0019

Table 3. Coefficients of V_{cmax} for Eq. [21]

Species	a_2	b_2	c_2
Aspen	-0.0050	-0.0048	-0.00017
Jack pine	-0.0139	-0.0046	-0.00011
Black spruce	-0.0074	-0.0046	-0.00014
White spruce	-0.0169	-0.0047	-0.00011

Table 4. Parameters of V_{cmax} for Eq.[22]

Species	ΔH_a	ΔS	ΔH_d
Aspen	23883	792	240871
Jack pine	28526	899	273437
Black spruce	25410	796	242404
White spruce	23690	889	269756
Average	25377	844	256617

Table 5. Parameters of V_{cmax} for Eq. [22], derived by holding

ΔH_d at 200000 and ΔS at 660.

Species	ΔH_a	ΔS	ΔH_d
Aspen	24059	660	200000
Jack pine	28910	660	200000
Black spruce	26179	660	200000
White spruce	23050	660	200000
Average	25549	660	200000

When Eq. [20] and Eq[21] were used to model the relationship between soil temperature

and V_{cmax}, there were no specific patterns in coefficients between different tree species

(Tables 2 and 3, Figures 5a to 5d). When Eq. [22] was used, the variation in ΔH_a, ΔH_d,

and ΔS was small among the four species (Table 4, Figures 5a to 5e). By holding ΔHd at

200000 and ΔS at 660 according to the values used in the dependency of V_{cmax} on leaf

temperature in Harley et. al. (1992) and Wohlfahrt et. al. (1998), ΔHa was re-estimated for the four species (Table 5, Figures 5a to 5d).

Eqs. [20], [21], [22] and [22] with ΔS = 660 and ΔH_d = 200000 fitted the measured V_{cmax} data well (Figure 5a-5e). For example, curve fitting the V_{cmax} for aspen with the three equations, the norm (depicting closeness of the fitting to measured data-points) for Eq.[20] was 31.31, for Eq.[21] was 40.64, Eq.[22] was 28.22, and Eq.[22] with ΔS = 660 and ΔH_d = 200000 was 32.28. Therefore, there was no big difference in the fitting effects of the three equations.

Among the four species, V_{cmax} for aspen were significantly higher than the other three conifers. V_{cmax} among the three conifers were not significantly different from each other (P = 0.05) (Figure 5e).
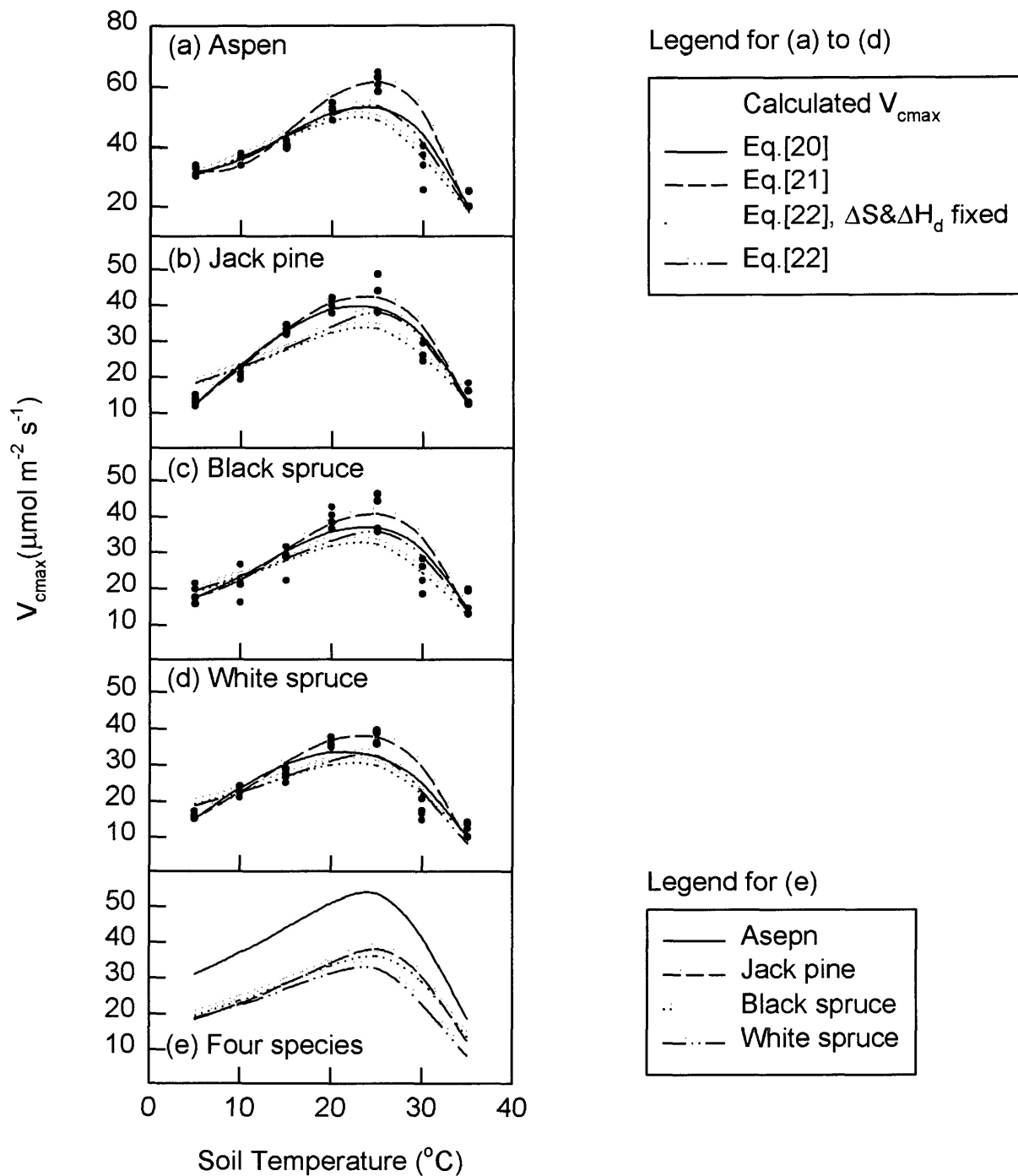
Figure 5. V_{cmax} vs. soil temperature for aspen, jack pine, black spruce and white spruce. Eq.[22] with corresponding parameter values in Table 4 was used for Figure. 5(e).

Effects of soil temperature on J_{max}

As might be expected, soil temperature affected J_{max} for the four species in the same manner as the soil temperature did on V_{cmax}, but the data for J_{max} showed a greater variability (Figures 6a to 6d).

The following equations were used to model the relationship between soil temperature and J_{max}:

$$J_{max} = a_3 + b_3 \cdot T_s + c_3 \cdot T_s^2 + d_3 \cdot T_s^3 \qquad [23]$$

$$J_{max} = J_{max\,25} \cdot [1 + a_4 \cdot (T_s - 25) + b_4 \cdot (T_s - 25)^2 + c_4 \cdot (T_s - 25)^3] \qquad [24]$$

$$J_{max} = \frac{J_{max\,25} \cdot e^{\left[\frac{\Delta H_a}{R \cdot 298} \cdot (1 - \frac{298}{T_s})\right]}}{1 + e^{\left[\frac{\Delta S \cdot T_s - \Delta H_d}{R \cdot T_s}\right]}} \qquad [25]$$

Where a_3, b_3, c_3, d_3, a_4, b_4, and c_4 are coefficients in Eq.[23] and Eq.[24]. In Eq.[25], ΔH_a is the activation energy, ΔH_d is the deactivation energy, ΔS is an entropy term, T_S is the soil temperature in °C or K according to the equations used, and R is the gas constant. J_{max25} is the mean value of J_{max} at 25 °C.

In general, J_{max} in each species increased exponentially with increasing soil temperature from 5 °C to the optimum temperatures (most of them were at 25 °C), then

decreased exponentially (Figures 6a to 6e). Coefficients for Eqs.[23] to [25] were listed in Tables 6 to 9.

Table 6. Coefficients of J_{max} for Eq. [23]

Species	a_3	b_3	c_3	d_3
Aspen	85.53	-3.91	0.59	-0.015
Jack pine	19.44	4.68	0.047	-0.0047
Black spruce	62.27	-3.58	0.57	-0.0136
White spruce	18.04	4.79	0.046	-0.00464

Table 7. Coefficients of J_{max} for Eq. [24]

Species	a_4	b_4	c_4
Aspen	-0.005	-0.004	-0.00013
Jack pine	-0.018	-0.003	-0.0000489
Black spruce	-0.003	-0.0046	-0.000158
White spruce	-0.011	-0.0040	-0.0000987

Table 8. Parameters of J_{max} for Eq. [25]

Species	ΔH_a	ΔH_d	ΔS
Aspen	20168	250926	821
Jack pine	16861	257233	840
Black spruce	26401	232804	765
White spruce	23719	224307	736
Average	21787	241317	790

Table 9. Parameters of J_{max} for Eq. [25], derived by holding

ΔH_d at 200000 and ΔS at 660.

Species	ΔH_a	ΔH_d	ΔS
Aspen	21905	200000	660
Jack pine	18733	200000	660
Black spruce	27350	200000	660
White spruce	24997	200000	660
Average	23246	200000	660

As it was the case with V_{cmax}, when Eq.[23] and Eq.[24] were used to model the effects of soil temperature on J_{max}, the coefficients showed no specific patterns among different species (Tables 6 and 7, Figures 6a to 6d). Similarly, as it was done with V_{cmax}, holding ΔH_d at 200000, and ΔS at 660 in Eq.[25], ΔHa for J_{max} for the four species were re-analyzed and the results were shown in Table 9 and Figures 6a to 6d.

J_{max} for aspen was chosen to check the fitting performance of the three equations: Eq.[23], [24] and [25]. The norm associated with Eq.[23] was 67.12, Eq.[24] 74.04, Eq.[25] 65.77, and Eq.[25] with fixed $\Delta S = 660$ and $\Delta H_d = 200000$ was 107.86. Considering relatively bigger values and greater variability for J_{max}, the norms for the three equations were not distinctively different. The three equations and Eq.[25] with ΔS = 660 and $\Delta H_d = 200000$ fitted the measured J_{max} data-points well (Figure 6a-6e). The norms for J_{max} were much bigger than those for V_{cmax} due to greater variability of J_{max} data.
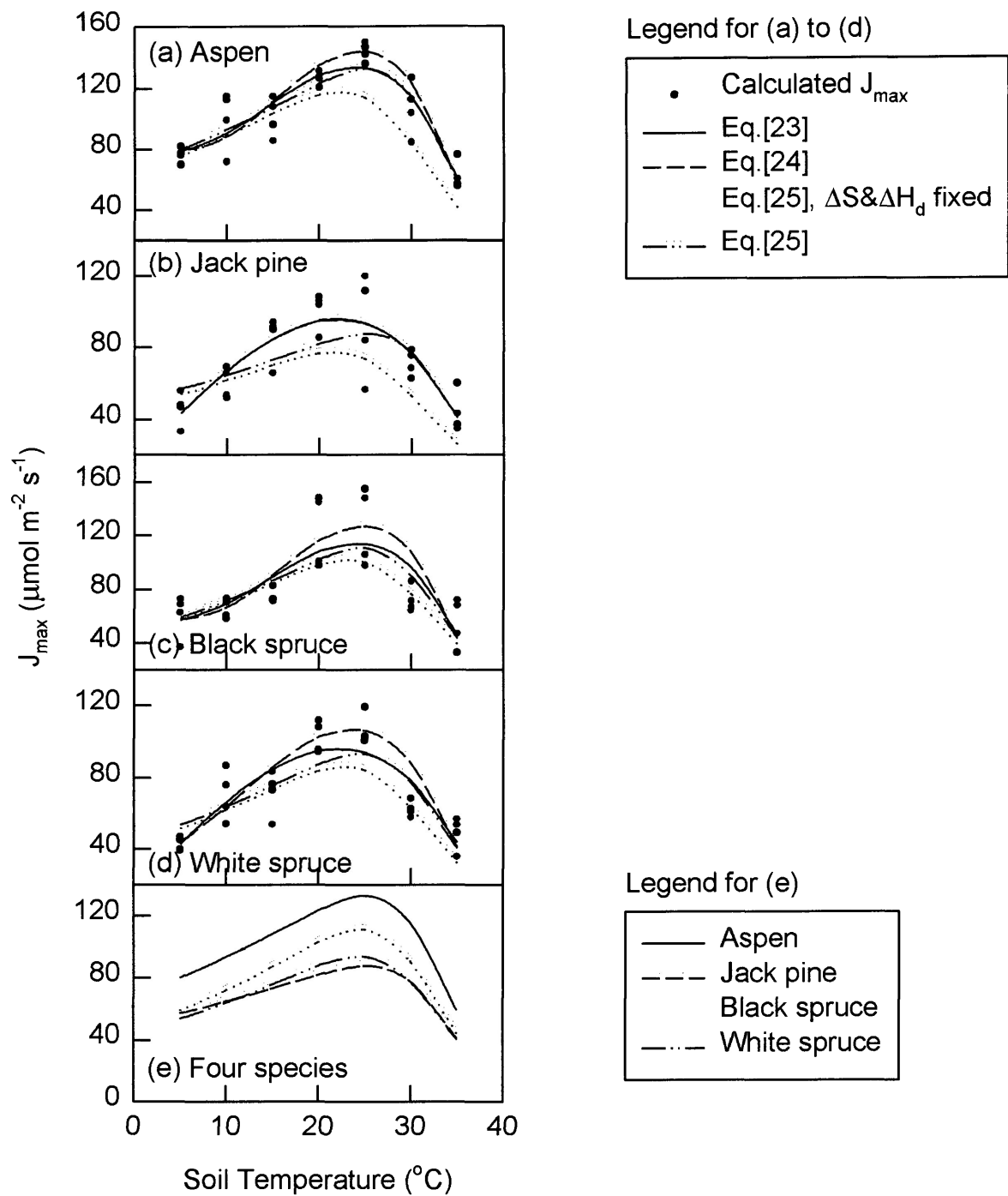
Figure 6. J_{max} vs. soil temperature for aspen, jack pine, black spruce and white spruce. Eq.[25] with parameter values in Table 8 was used for Figure 6(e).

J_{max} values for aspen were significantly higher than the values for the three

conifers ($P = 0.05$). J_{max} values for white spruce and jack pine was not significantly

different from each other, but J_{max} values for black spruce were significantly smaller than

those for white spruce and jack pine. This was in contrast to the situation for V_{cmax}, where

there was no significant difference between the three conifers.

Wullschleger (1993) investigated 109 different species and found that there

existed a strong correlation between V_{cmax} (the Rubisco limited rate of carboxylation) and

J_{max} (the light saturated rate of electron transport). In this study, the relationship between

V_{cmax} and J_{max} was examined for all four species together through regression. The

resultant relationship agreed well with the one proposed in Wullschleger (1993) and

Leuning (1997) (Figure 7).

Effects of soil temperature on R_d

R_d, the daytime (in light) non-photorespiratory CO_2 evolution continuing in the

light, derived from the linear part of light response curve, were not significantly different

both among the four boreal tree species and among the seven different soil temperatures

in each species ($P = 0.05$).

The R_d value ranged from 0.01 to 1.5, but most of the data concentrated in the

range of 0.3 to 0.9. The results agreed well with the R_d values in Kirschbaum and

Farquhar (1984), Brooks and Farquhar (1985) and Harley et al (1992). The average value

of R_d for all the four species across all the soil temperatues was 0.53 $\mu mol\ m^{-2}\ s^{-1}$ (Figure

8.).

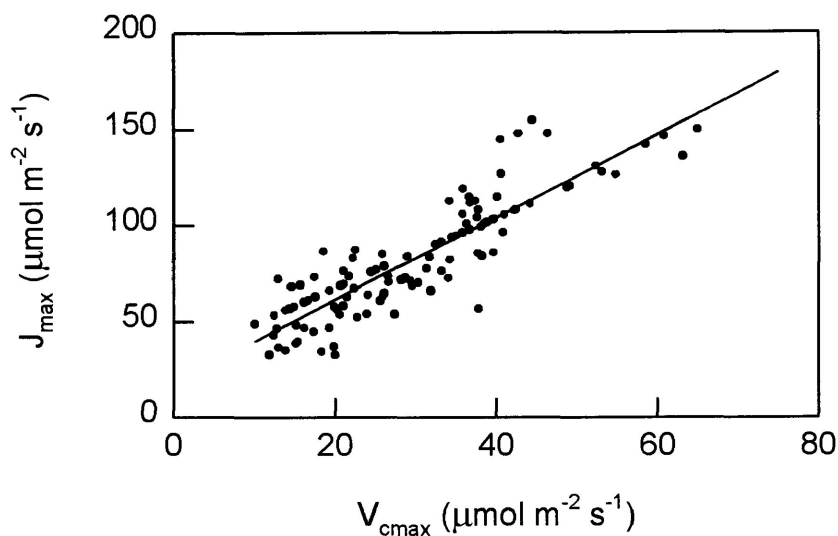Figure 7. Relationship between V_{cmax} and J_{max}. The line
represents the linear regression between V_{cmax} and J_{max}:
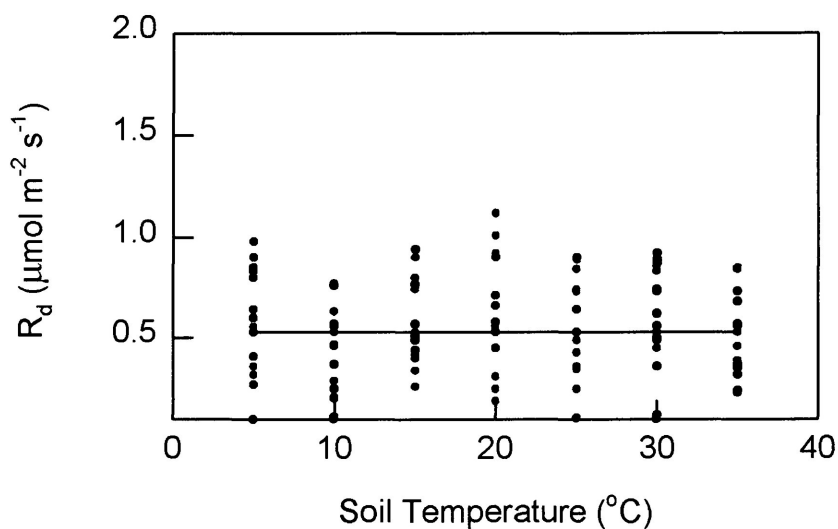$$Jmax = 2.15{*}V_{cmax} + 18.39 \ (R^2 = 0.78).$$

Figure 8. R_d vs. soil temperature. Data were pooled together
for all the four species and seven soil temperatures. The line
represents the average R_d = 0.53 for the four species across all the
soil temperatures.

Effects of soil temperature on α

α was derived from the initial part of the light response curve of photosynthesis (PAR < 200 μmol m^{-2} s^{-1}). The α values showed big variability both for different soil temperature and different tree species (data not shown). Data presented in Figure 9 were pooled α values for the four species at each soil temperature. The following two equations were employed to model the relationship between soil temperature and average α at each soil temperature.

$$\alpha = \alpha_{25} \cdot [1 + a_5 \cdot (T_s - 25) + b_5 \cdot (T_s - 25)^2 + c_5 \cdot (T_s - 25)^3] \qquad [26]$$

$$\alpha_{max} = \frac{\alpha_{25} \cdot e^{\left[\frac{\Delta H_a}{R \cdot 298} \cdot (1 - \frac{298}{T_s})\right]}}{1 + e^{\left[\frac{\Delta S \cdot T_s - \Delta H_d}{R \cdot T_s}\right]}} \qquad [27]$$

Where a_5, b_5, c_5 are coefficients in Eq.[26] and ΔH_a, ΔH_d and ΔS denote activation energy, deactivation energy and an entropy term respectively in Eq. [27]. The coefficients and parameters for Eqs. [26] and [27], including the ΔH_a value by fixing $\Delta H_d = 200000$ and $\Delta S = 660$, were shown in Table 10.

Table. 10. Parameters and coefficients for Eqs. [26] and [27].

a_5	b_5	c_5
-0.0099916	-0.0014968	-0.0000113
ΔH_a	ΔS	ΔH_d
8651.79	529.13	164677
10430	660	200000

The average α value at 20 and 25 °C (0.22) were very close to the values used in Harley et al. (1992) and Harley&Baldocchi (1995) for plants under no environmental stresses.

The norms (squared SS value for evaluating the performance of the above two equations) for α with Eqs.[26], [27], and [27] with ΔS = 660, ΔH_d = 200000 were 0.03, 0.04 and 0.06 respectively. Eqs.[26] and regular [27] fitted the average α well, but Eq.[27] with ΔS = 660, ΔH_d = 200000 did not fit the average α as well as the first two cases, especially at 35 °C (Figure 9).

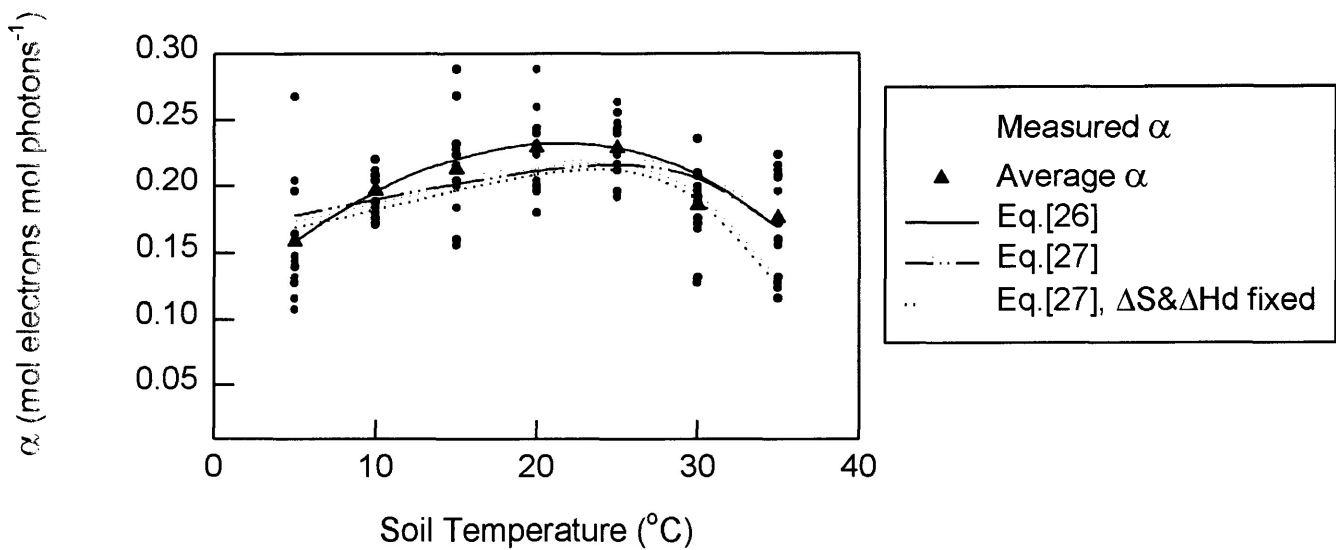Figure 9. α vs. soil temperature. Data were pooled together for all the four species. Curves represent average α for each soil temperature modeled by different equations.
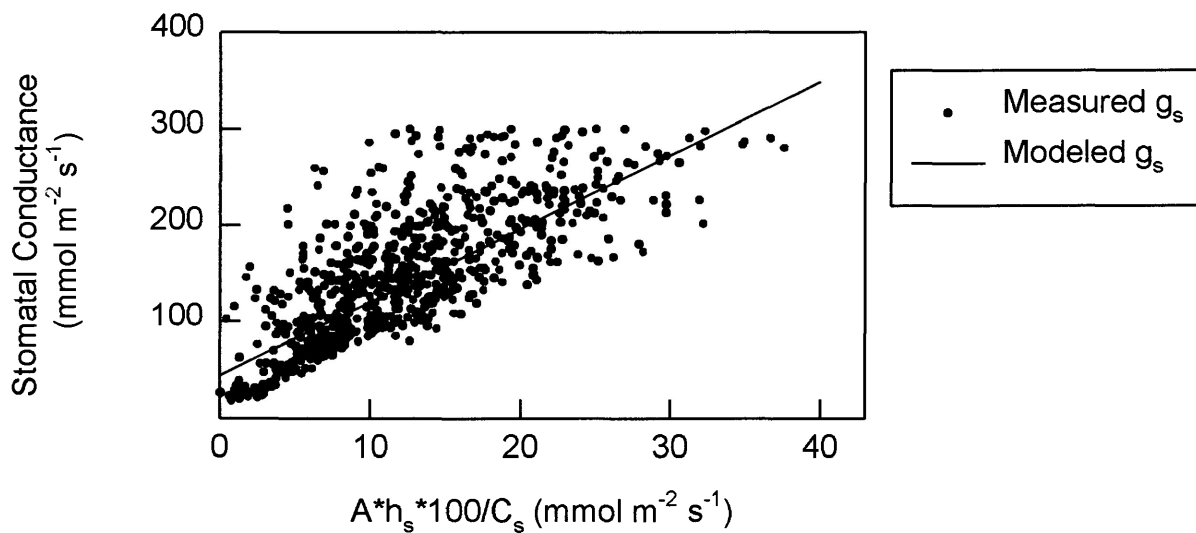

Figure 10. Relationship between measured stomatal conductance and the product of $(A^*h_s^*100/C_s)$. The solid line represents the linear regression: Measured $g_s = 44.21 + 7.61^*A^*h_s^*100/C_s$ ($R^2 = 0.57$).

Effects of soil temperature on conductance model

For each soil temperature treatment, stomatal conductance data were pooled from a large number of gas exchange measurements for each species, in which stomatal conductance varied in response to leaf temperature, CO_2 and PAR. Leaf conductance to water vapor was plotted versus $A \cdot 100 \cdot h_s/C_s$, and the intercept (b) and the slope (m) were determined by linear regression (Table 11). As suggested by Ball et al. (1987) and Harley et al. (1992), data with C_a below 30 Pa or PAR below 150 μmol^{-1} m^{-2} s^{-1} were not used to estimate b and m in Eq. [16]. The Ball et al. (1987) empirical model of stomatal conductance, even though frequently used, has been criticized, because it is widely accepted that stomatal conductance responds to water vapor pressure (VPD) rather than to leaf surface relative humidity (Aphalo and Jarvis 1991). Leuning (1990, 1995) replaced surface relative humidity with a hyperbolic function of VPD and C_s with C_s- Γ_*, but his contribution did not significantly improve the model performance, so in this study the original stomatal model (Ball et al. 1987) was still employed.

When the model was parameterized separately for each species, m ranged from 3.16 to 11.9 and b ranged from 7.43 to 108.47. When all the data were pooled together, m = 7.61, and b =44.21 (Figure 10). The m and b values in Table 11 agreed with the corresponding values in Harley et. al. (1992) and Wohlfatrt et. al. (1998).

Since Eq.[16] is an empirical equation plus the complexity of stomatal behavior and large differences in R^2 values between the four species and between the seven soil

temperatures, no attempt was made to statistically compare the m and b values for the

four species and the seven soil temperatures. The relationship in Figure 10:

Measured g_s = 44.21 + 7.61·A·h_s·100/C_s can be empirically applied to any soil

temperature.

Table 11. Stomatal conductance model parameters (Eq.[16]) for the four species and the

seven soil temperatures.

°C		Aspen	Jack pine	Black spruce	White spruce
5	m	11.9	9.89	5.94	3.16
		24.01	7.73	32.60	50.41
		11.1	6.71	7.48	6.3
		53.74	34.10	23.16	40
		6.18	3.66	6.99	5.1
		82.95	115.29	61.27	72
20		9.86	6.69	8.36	3.71
		87.21	72.56	78.18	36
25		8.8	5.97	8.67	6.29
		64.51	68.43	35.53	15.55
30		7.87	5.52	8.54	9.16
		25.08	88.16	37.73	42.34
		9.26	2.54	3.73	8.78
		15.06	108.47	81.68	68.26

Model validation

Because most of the data collected in this study were used in parameterizing the

model, a true validation against an independently measured data set was not possible.

However, pooling the data, where C_a, PAR, soil temperature and humidity all varied, and

comparing measured values of net CO_2 assimilation, stomatal conductance and C_i with

values predicted by the model, the ability of the model to simulate measured data can be

visually assessed (Figure 11). Model predictions were obtained as follows. Inputs to the

model included measured C_a, PAR, leaf temperature, relative humidity, soil temperature,

modeled V_{cmax} and J_{max} at each specific soil temperature in Eq.[22] and Eq.[25], α in

Eq.[27], R_d, bio-chemical parameters (e.g., K_c, K_o, τ and their appropriate temperature

parameters in Table 1.) and the appropriate slopes and intercepts of the leaf conductance

in Table 11. For each set of inputs, the model then iterated for the C_i value which

satisfied Eqs. [6], [16], and [17] simultaneously. When the initial assumed C_i and that

calculated in Eq[17] agreed to within 0.01 Pa, the iteration was concluded. The calculated

C_i, A and g_s were then compared with measured values.

The photosynthesis and C_i predicted by the models were very close to the

measured values (Figure 11a and 11b), but the relationship between measured and

predicted g_s was not nearly as tight as that for photosynthesis and C_i (Figure 11c).
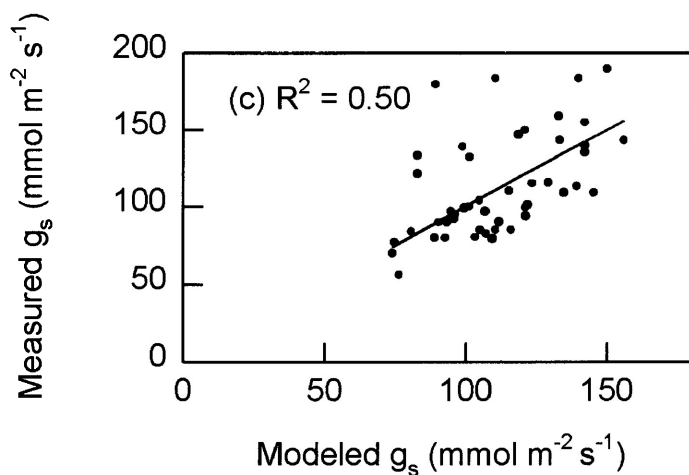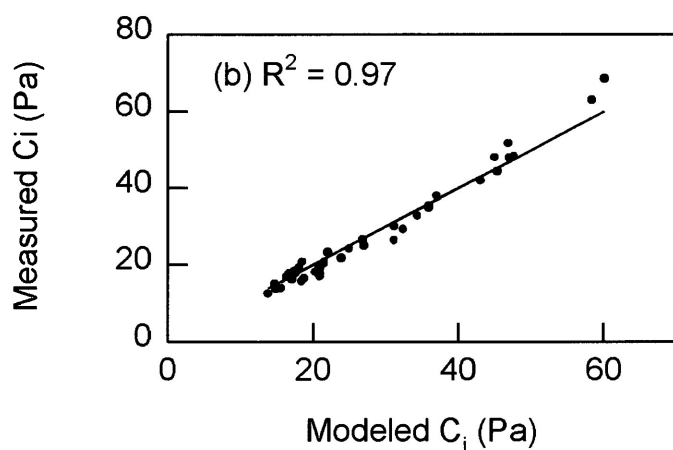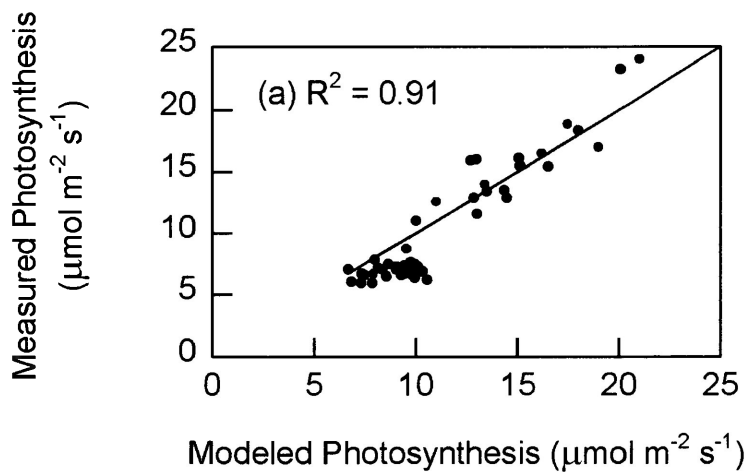
Figure 11. Comparison of measured net A, g_s and C_i with values modeled by the model. Lines are 1:1 lines. The data in Figure 11(a), (b) and (c) are from black spruce 10 °C, white spruce 25 °C, and aspen 5 °C.

Model Simulation

Using the V_{cmax} values in Figure 5e, J_{max} values in Figure 6e, corresponding α values in Eq. [27], and with fixed $R_d = 0.53$ (Figure 8) and $T_L = 22\,^\circ C$, the A/C_i curves for the four species across the seven soil temperatures were simulated (Figures 12a to 12d).

The modeled A/Ci curves showed that the seven soil temperatures could roughly be broken into four groups: 5 $^\circ$C and 35 $^\circ$C; 10 $^\circ$C and 30 $^\circ$C; 15 $^\circ$C; 20 $^\circ$C and 25 $^\circ$C. Soil temperatures of 20 $^\circ$C and 25 $^\circ$C had the highest A/C_i curves, while 5 $^\circ$C and 35 $^\circ$C were associated with the lowest A/C_i curves among the seven soil temperatures.
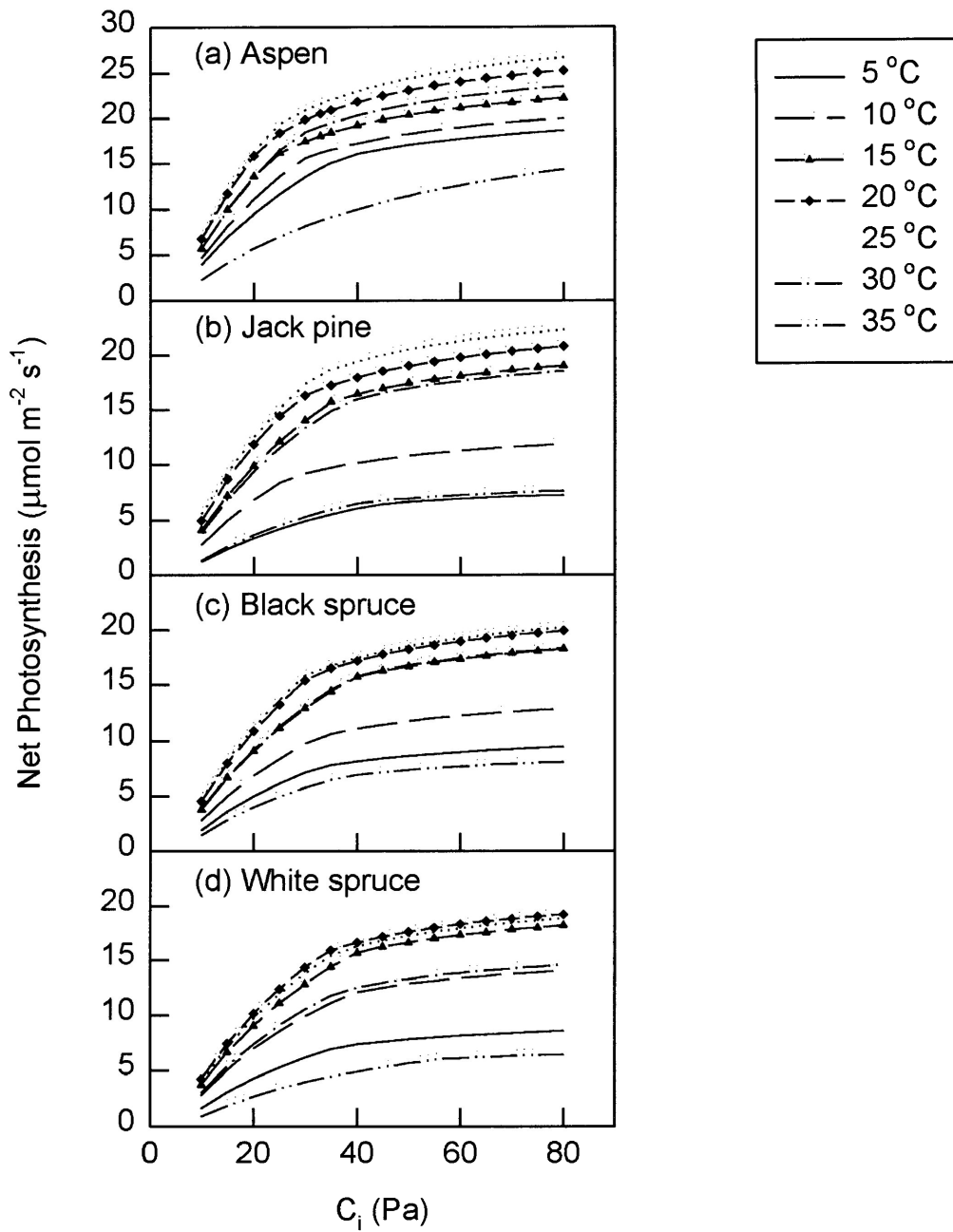
Figure 12. Modeled A/C$_i$ curves for Aspen, Jack pine, Black spruce and White spruce across the seven soil temperatures.

DISCUSSION

Temperature symmetry

It was hypothesized in the Introduction that the four boreal trees had dual

temperature symmetry. The first hypothesis to test in this regard (i.e., above-ground and

below-ground temperature symmetry) was that, if the leaf temperature was kept constant,

and the soil temperature was increased from 5 °C to 35 °C, V_{cmax} (or J_{max}) would increase

(or decrease) exponentially in the same pattern with soil temperature as if the soil

temperature were kept constant, and the leaf temperature were increased from 5 °C to 35

°C. The data of this paper showed that the corresponding ΔS and ΔH_d values for both the

leaf temperature equation (Eq.12.) and soil temperature equation (Eqs.[22] and [25]) were

very similar. If ΔS and ΔH_d were fixed at $\Delta S = 660$ and $\Delta H_d = 200000$, the only

difference between the two equations was ΔH_a. The ΔH_a values for both V_{cmax} and J_{max} in

Eqs.[22] and [25] were smaller than the value in Eq. [12] (Compare Tables 5 and 9 with

Table 1).

Soil temperature may have affected the photosynthetic machinery by its impacts

on root enzymatic activities, root cell membrane permeability, osmotic potential and

viscosity of soil solution (Ting 1982). All these mechanisms could have affected nutrient

absorption, water uptake and transport (Camm and Harper 1991; Kaspar et al. 1992;

Raich and Schlenger 1992; Ciais et al. 1995), but the impact of soil temperature on V_{cmax}

and J_{max} was more indirect compared with that of leaf temperature, which may explain

the lower soil temperature dependency (i.e., lower ΔH_a). Nonetheless, Figure 13 provided

evidence to support the above and below ground temperature symmetry hypothesis, but the optimum soil temperature for photosynthetic parameters was lower than the corresponding optimal air temperature.

Figure 13 also supported the low and high temperature symmetry, but the symmetry was not that clear-cut and perfect, with a steeper slope at the high temperature range than at lower temperatures. The steeper slope at high temperatures indicated that high temperatures were more detrimental to the photosynthetic machinery than low soil temperature. This was in line with the observation of the high mortality in white spruce and black spruce at high soil temperatures, e.g.,49.3% and 62.5% respectively at 30 ^{o}C, and nearly 90% for both species at 35 ^{o}C. But no mortality was observed at low soil temperatures for any of the four species. High temperature damage might have resulted from ion leakage , the liquefaction of protein lipids and the denaturation of proteins , and increases in toxic compounds in the root system (Kozlowski et. al. 1991). However, the exact mechanisms causing the deviation from symmetry are not clear.

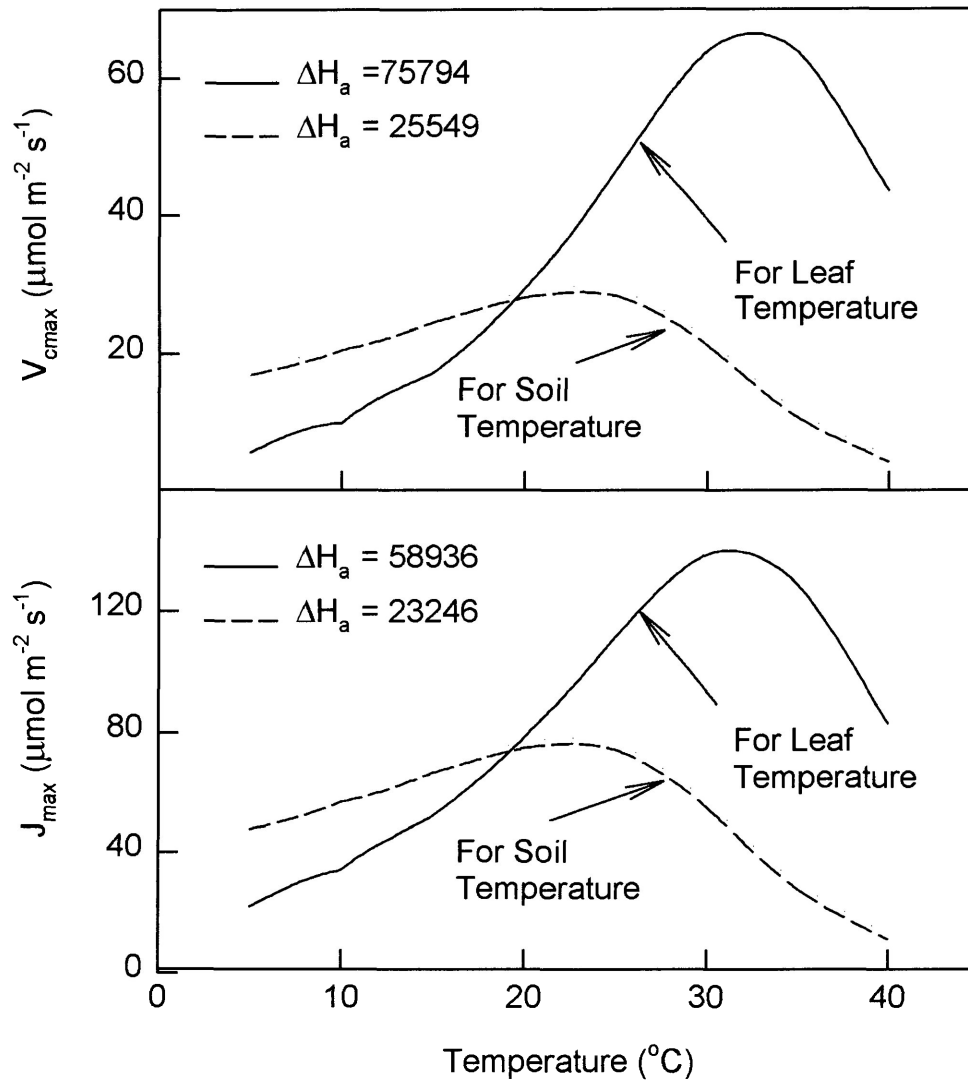Figure 13. Temperature dependencies of V_{cmax} and J_{max}.
ΔH_a values for leaf temperature were from Table 1 and
ΔH_a values for soil temperature from Tables 5&9. ΔH_d
and ΔS were held at 200000 and 660 respectively.

Soil Temperature vs. V_{cmax}, J_{max} and α

Despite of the relatively large amount of information on soil temperature effects in the literature, comparative studies on the response of several species to a wide range of soil temperatures are rare. Furthermore , most studies expose trees to a small range of soil temperatures, such as 3 to 15 °C for black spruce (Landhaauser et al. 1996), 3 to 11 °C for white spruce (Harper and Camm 1993). Even though the effects of soil temperature in the literature are often confounded with those of ambient air temperature because of the difficulty in controlling soil temperature independently of air temperature (Nielsen and Humphries 1996), the results in this study agreed with the results in the literature (Heninger and White 1974; Lawrence and Oechel 1983; Landhaausser et al. 1996).

Soil temperature can impact V_{cmax}, J_{max} and α through its impacts on nutrient uptake, especially nitrogen absorption. V_{cmax} reflects nitrogen investment in Rubisco, J_{max} reflects nitrogen investment in the two photosystems of photosynthesis and α represents nitrogen investment in light harvesting pigments. These parameters were all highly correlated to the leaf nitrogen level (Evans and Seemann 1989; Niinemets and Tenhunen 1997). Even though ample nutrients were applied over the course of the experiment (cf. Growing Conditions), the seedlings might have had different nitrogen concentration in their foliage due to the effects of different soil temperature on nutrient uptake. The leaf nitrogen level in this study was not measured, but it could visually be assessed by leaf color. The leaf color for the four species at 5 °C and 35 °C was very yellowish compared with that at 25 °C, which may be one of the factors responsible for the lower parameter values (e.g., V_{cmax} and J_{max}) at extremely low and high soil temperatures.

The apparent quantum yield of photosynthesis is extremely constant for all

non-stressed C_3 species and usually taken as 0.073 mol CO_2 (mol quanta) $^{-1}$

(Ehleringer&Björkman 1977, Sharkey 1985, Harley et al. 1992). The assumption that 4

mol electrons are required to regenerate enough RuBP for the carboxylation of 1mol CO_2

gives an equivalent value of 0.292 (i.e., 0.073*4) mol electrons (mol quanta) $^{-1}$ However,

C_3 leaves utilize light with a lower efficiency in natural environments because of the less

than 100% absorption of PAR and energy dissipation by non-photophosphoration

processes. The actual α is the product of 0.292 and leaf absorption

(α = 0.292*leaf absorption) (Niinemets and Tenhunen 1997). The typical leaf absorption

is 86%, and therefore the frequently used α value in modeling is around 0.24. Leaf

absorption is assumed to depend on leaf chlorophyll content (Niinemets and Tenhunen

1997). Figure.9 showed that average α increased slightly with soil temperature from 5 °C

to 25 °C, then decreased to 35 °C. The change of α with soil temperature may be related

to different leaf chlorophyll contents under different soil temperatures. Non-

photochemical dissipation of light energy also increases as the environmental conditions

become stressful (Demmig-Adams and Adams 1992).

R_d vs V_{cmax}

Although the relationship between mitochondrial respiration and photosynthesis in chloroplasts is fairly complex, positive relationships between light saturated photosynthesis and respiration are often observed (Walters & Field 1987; Ceulemans & Saugier 1991). Assuming that the respiratory cost for leaf is directly related to the physiological activity of the foliage, the respiration rate of leaves is often taken as a proportion of V_{cmax} (Collatz et al. 1991; Sellers et al. 1996; Niinemets & Tenhunen 1997; Wohlfahrt et al. 1998). The coefficients of the relationship between V_{cmax} and R_d used in the above literature ranged from 0.0052 to 0.038. In this study, the Rd was regressed against V_{cmax}, (Figure 14), but showed no significant relationship. However, the coefficient from Collatz et al. (1991) appears to be reasonable for describing our data (Figure 14).

There is still considerable controversy about the magnitude of R_d. Some results suggested that it might be totally inhibited in light (Forrester et al. 1966; Laing et al. 1974) while others suggested that it was a variable fraction of R_{dark} (Heath & Orchard 1968; Poskuta 1968; Azcon-Bieto et al. 1981; Peisker et al. 1981; Brooks and Farquhar 1985). Peisker et al. (1981) concluded that the ratio of R_d/R_{dark} varied during ontogenetic development, was averaged about 0.6, but with extremes of 0.25 and 0.8. Compared to the literature, the assumption of $R_d/R_{dark} = 0.5$ in this study may seem reasonable.
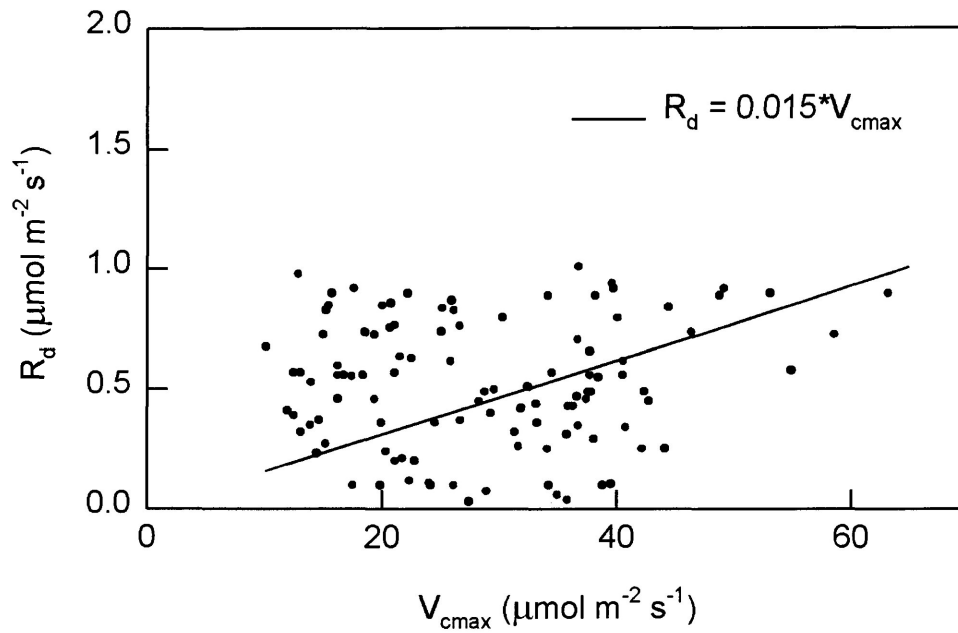
Figure 14. R_d vs. V_{cmax}. The R_d and V_{cmax} data were pooled
together for all the four species and seven soil temperatures.
In this study, R_d and V_{cmax} did not have a linear relationship.
The line $R_d = 0.015*V_{cmax}$ was from Collatz et al. (1991).

Currently there are several ways to determine R_d. One way (Method 1) is through non-linear regression for the initial part of the A/C_i curve using Eqs. [6] and [7] with data collected at saturating PAR and C_i values less than 25 Pa. Thus, the V_{cmax} and R_d can be determined simultaneously (Harley et al. 1992). Another way (Method 2) calculates R_d as A at the CO_2 compensation point Γ_* from the regression for the initial part of A/C_i curve using data as in Method 1 (Kirschbaum and Farquhar 1984; Harley & Baldocchi 1995). The last approach (Method 3) is to linearly regress the initial part of light response curve and take the intercept as R_{dark} (Wohlfahrt et al. 1998; Falge et al 1996) and R_d is assumed to be half the magnitude of R_{dark}. Method 3 is the method used in this study. The R_d values determined by the three methods for seven A/C_i and their corresponding light response curves were shown in Table 12. Even though the values were quite variable, they all fell within a reasonable range. Table 12 suggested that any of the three methods can be used for calculating R_d.

Table 12. Comparison of R_d values determined by three different methods.

Method	R_d values						
Method 1	0.11	0.85	0.69	1.29	0.16	0.39	0.47
Method 2	1.02	0.02	0.43	0.54	0.20	0.51	1.33
Method 3	0.49	0.57	0.33	0.71	0.35	0.88	0.76

In order to test the effect of R_d values estimated using different methods on the calculation of V_{cmax} and J_{max}, R_d values were fixed at 0.5, 1.0, 1.5, 2.5, 4.0, and 7.0. At each R_d value, V_{cmax} and J_{max} were estimated using the SigmaPlot curve-fitting program.

The parameter estimation protocol was described in Model Parameterization. For each R_d, the program was always able to find corresponding V_{cmax} and J_{max} values which fit the measured A/C_i curve well (Figure 15a to 15c).

Different R_d values affected the calculation of V_{cmax} and J_{max} (only V_{cmax} shown in Figure 15d). But if the R_d value fell in its reasonable range (0-1.5), the effect was small and within the experimental error in this study (ANOVA Table not shown) (Figure 15d). So by following this line, setting R_d at its mean value (0.53) in Model Simulation seemed justifiable.
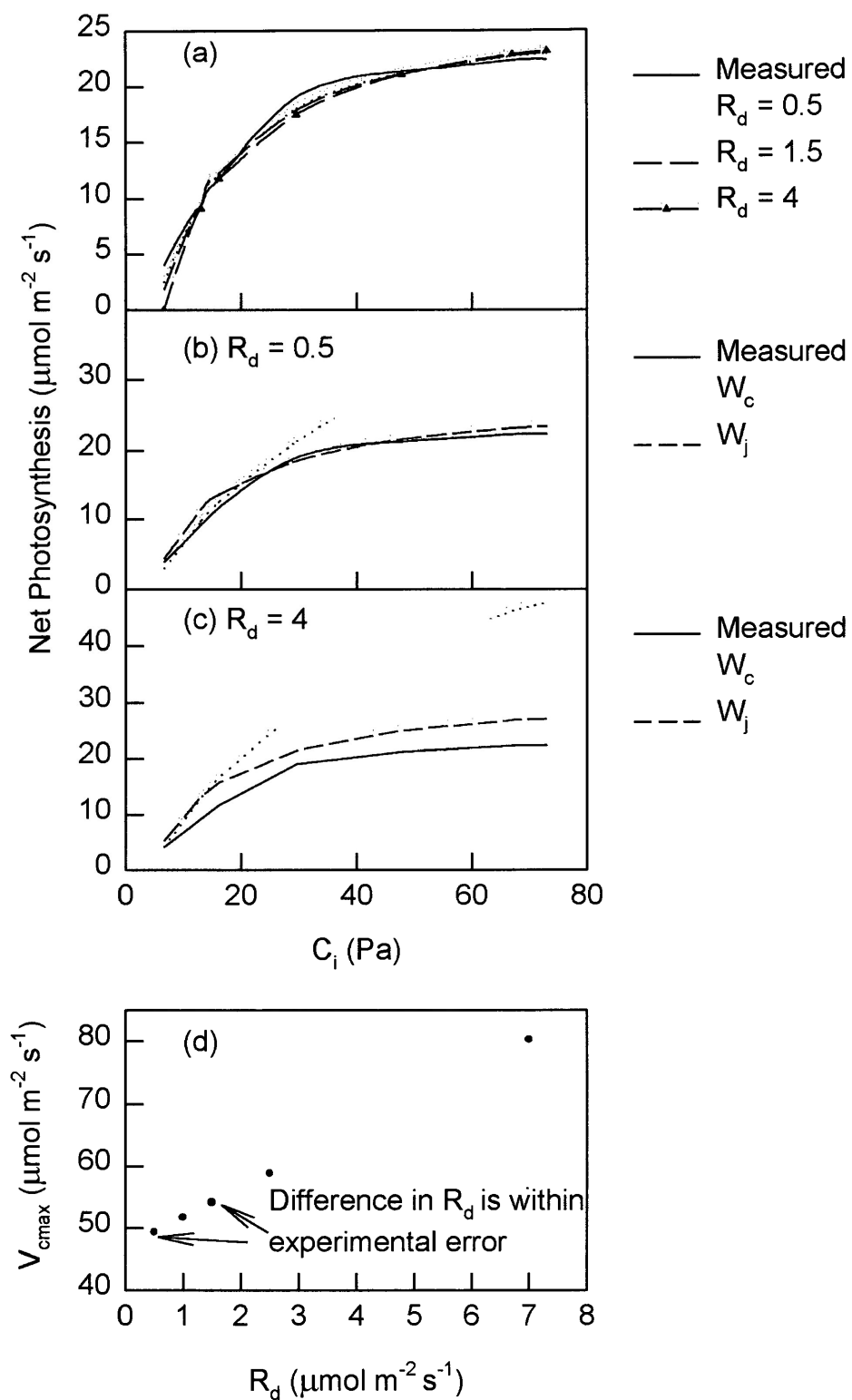
Figure 15. The effect of different R_d values on V_{cmax} for a measured A/C_i curve. Despite different R_d values, there are always corresponding V_{cmax} and J_{max} that fit the measured A/C_i curve well.

Acclimation strategies to soil temperature

The data in this study suggested that the four species may have adopted two strategies to acclimate to different soil temperatures, especially to extreme soil temperatures (eg. 5 °C and 35 °C). One strategy is to optimize nitrogen investment and the second strategy is to balance water cost and nitrogen benefit.

The relationship between V_{cmax} and J_{max} in this study (Figure 7) was very similar to the one developed by Wullschleger (1993). Despite different rates of assimilation and soil temperatures, the four species maintained a close balance in the allocation of resources to these two functional components. A similar observation was noted in a study of four tropical species by Thompson et al. (1992) who showed a tight coupling of V_{cmax} and J_{max} for leaves grown under different light and nutrient regimes. This result suggests that the four boreal trees were able to optimize the allocation of resources, particularly nitrogen across a wide range of temperature conditions, in order to preserve a balance between enzymatic (i.e., Rubisco) and light-harvesting (i.e., chlorophyll) capabilities.

Stomatal conductance to the diffusion of water vapor and CO_2 is a compromise between the promotion of carbon assimilation and the diminution of water loss (Cowan 1977; Raschke 1979; Farquhar et al. 1980). This compromise is effective if stomata tend to open in response to conditions that favor rapid assimilation of carbon and to close in response to conditions that favor rapid transpiration. The interesting phenomenon is, despite under different soil temperatures, the four species operated photosynthesis in such a way that it was approximately co-limited by W_c and W_j (Figure 16.).

A higher stomatal conductance and corresponding higher C_i values beyond the co-limited points (arrows in Figure 16.) would only marginally increase CO_2 assimilation, but would result in significant increase in transpiration, because transpiration increases linearly with g_s (Figure 17.). Below the co-limited points, photosynthesis does not decline as fast as transpiration does with decreasing g_s. Thus, decreasing g_s and C_i are coupled with an increasing water use efficiency (WUE) (carbon gain per water lost). However, decreasing g_s will result in less of the total photosynthetic capacity being used, which would lead to a reduced photosynthetic nitrogen use efficiency (PNUE) (carbon gain per unit leaf nitrogen). As a result, the co-limited point is a compromise between the efficient use of water and the efficient use of nitrogen in the photosynthetic machinery (Lambers et al. 1998).

The four species optimized nitrogen allocation in the different components of photosynthetic machinery (Figure 7.) and operated their photosynthesis at the point, which maximized the return (carbon gain) of water and nitrogen investment (Figure 16.). The results suggested that the photosynthetic mechanisms of the four species had acclimated to the different soil temperature after four months of treatment. According to Lambers et al. (1998), the bio-chemical acclimation of plant physiological processes generally occurs within days to weeks.
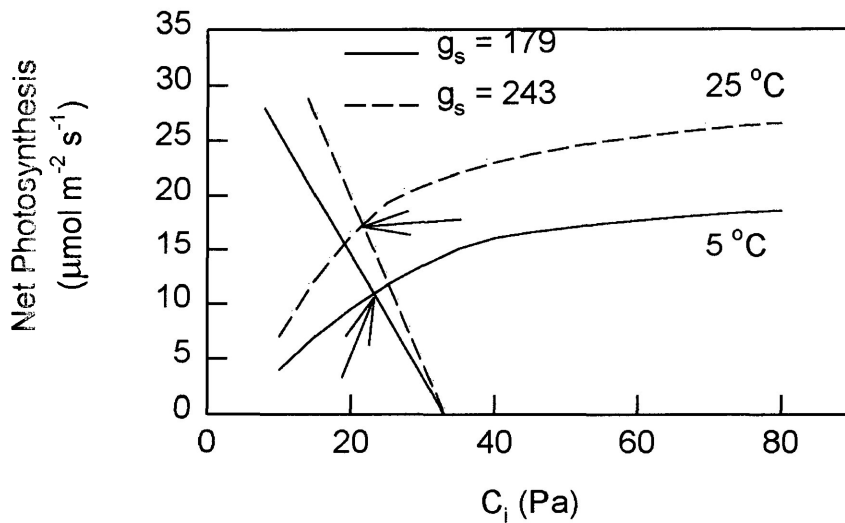
Figure 16. Relationship between net A and C_i for aspen.

A operates at the points (indicated by arrows) co-limited by W_c and W_j. To aviod overlaps between lines, only the A/C_i curves for 5 and 25 °C were presented.

The results for conifers and other temperatures were similar to the relationship in this figure.
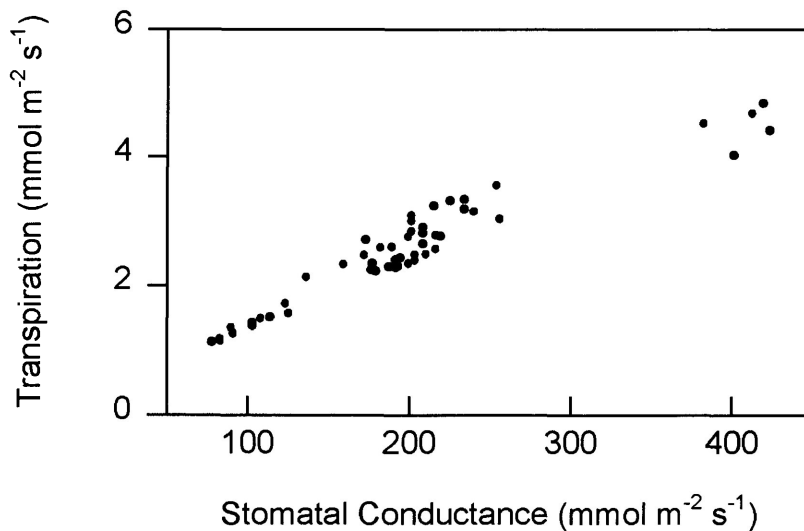

Figure 17. Transpiration (E) vs. stomatal conductance (g_s).

E increased linearly with g_s. Data shown here were the measured data for aspen at 25 °C soil temperature under different PAR and C_a.

The results for other soil temperatures and the conifers were similiar to the relationship in this figure.

Implication on silvicultural practice

The four boreal species have wide natural distributions in North America. Aspen ranges widely from 21 to 68 N, the spruces generally distribute from 42 to 69 N, reaching Mackenzie District in the Northwest Territories. Jack pine ranges from 42 to 60 N (Burns and Honkala 1990). In Yukon and Northwest Territories, the boreal species grow over permafrost with a layer of wet feather mosses from 25 to 46 cm in depth (Burns and Honkala 1990).

Mixed- woods are the most productive type of boreal forest and often consist of the four species (Burns and Honkala 1990). This paper concluded that the four boreal species had similar cardinal soil temperatures for key model parameters (i.e., the minimum, optimum and maximum soil temperatures for V_{cmax}, J_{max} and α). The boreal forest is characterized by its cold continental climate. For example, the average July soil temperature is about 15 °C in the boreal forest of Ontario (Stathers and Spittlehouse 1990). So most of the boreal forest is growing under sub-optimal soil temperature.

Soil temperature can be altered by silvicultural treatments, such as drainage of wetlands (Burns and Honkala 1990), scarification and plowing (Buse and Bell 1992), mounding and prescribed fire (McMinn 1982; Sutton 1984; Brand 1990) and ripping (Fleming et al. 1998). Prescribing silvicultural treatments to raise the boreal forest soil temperatures from its sub-optimal level to close to its optimal level can promote the productivity and growth of the boreal forest.

CONCLUSIONS

Soil temperature significantly affected parameters of the C_3 photosynthesis-stomatal conductance model, i.e., V_{cmax}, J_{max} and α. The three parameters showed exponential relationship with soil temperature and had dual temperature symmetry (above-ground and below-ground temperature symmetry, and low and high temperature symmetry). The four tree species, despite their wide natural distribution range, had similar cardinal soil temperatures for the above parameters. Model parameters performed best at the optimum soil temperature (20 and 25 $^{\circ}$C), poorest at stressful soil temperature (5, 35 $^{\circ}$C), and with 10, 15 and 30 $^{\circ}$C in between.

The four species, after four months of soil temperature treatment, acclimated to the wide range of soil temperature by optimizing their nitrogen investment into different photosynthetic components (V_{cmax} vs. J_{max}) and balancing their nitrogen and water use efficiency (PNUE vs. WUE).